

Fabrication and characterization of $\text{YBa}_2\text{Cu}_3\text{O}_7$ step-edge Josephson junctions prepared on sapphire substrates

Hae-Ryong Lim^{a,b*}, In-Seon Kim^a, Dong Ho Kim^b, Yong Ki Park^a, and Jong-Chul Park^a

^aKorea Research Institute of Standards and Science, P.O. Box 102, Yusong, Taejeon 305-606, Korea

^bDepartment of physics, Yeungnam University, Kyungsan 712-749, Republic of Korea

Received 7 February 2000

Abstract

Step edge Josephson junctions in *c*-axis oriented $\text{YBa}_2\text{Cu}_3\text{O}_7$ films were fabricated on CeO_2 buffered sapphire substrates. The step angle was controlled in the wide range of $20^\circ\sim 75^\circ$ by the Ar ion milling technique. *I-V* curves of junction fabricated on the thickness ratio of ~ 0.8 and the step angle of 35° were exhibited *RSJ*-like behavior with $I_C R_N$ product of $\sim 250 \mu\text{A}$ and critical current density of $\sim 2 \times 10^4 \text{ A/cm}^2$ at 77 K. Critical current of step edge junction was increased linearly with decreasing temperature but the normal resistance was almost constant. Total samples of step edge Josephson junction was satisfied a scaling behavior of $I_C R_N \propto (J_C)^{0.5}$.

Keywords : Step edge junction, YBCO, sapphire substrate, CeO_2 buffer layer.

I. Introduction

Step edge weak links in *c*-axis oriented $\text{YBa}_2\text{Cu}_3\text{O}_7$ (YBCO) films can be used for high temperature Josephson junction device operating at 77 K. High-Tc Josephson junction technology and superconducting quantum interference devices (SQUID) based on step edge junctions have been investigated by a large number of groups [1~12]. Step edge junctions have attracted a merit due to the free position of step, the low cost and the easy of fabrication process, and the low $1/f$ noise [13]. Step edge junctions have been fabricated on various substrates of SrTiO_3 [1,7,8,12], LaAlO_3 [4,10,12], MgO [2,11], and sapphire [3,9]. Sapphire substrate is of considerable interest in view of its modest dielectric constant and its commercial availability in large diameter substrate at low cost, compared with the other oxide single crystal substrates commonly used in high-Tc superconductor thin films deposition.

However, buffer layer is necessary in order to prevent reaction between sapphire substrates and high temperature oxide superconducting films, and to permit the oxide superconducting films to grow epitaxially. STO [14], MgO [15,16], YSZ [17~19] and CeO_2 [16, 20~21] have been investigated for the buffer layers. Among them, CeO_2 has been shown to be excellent as buffer layer of *r*-plane sapphire substrates. During the last years, encouraging results have been reported on the CeO_2 buffered sapphire substrates.

In this paper, we report the results of the characteristics of step edge Josephson junctions on CeO_2 buffered sapphire substrates prepared with the various step angles and the thickness ratios of YBCO thin film to the step height.

II. Experiments

Step-edge junctions were fabricated on $6 \text{ mm} \times 6 \text{ mm}$ *r*-plane sapphire substrates. First, 15-nm-thick Au film was deposited on substrate by *rf* sputtering

*Corresponding author. Fax : +82 42 868 5475
e-mail : hrlim@kriss.re.kr

method to enhance the clearness of the PR mask. The steps were fabricated by Ar-ion milling through photoresist (PR) mask. The step height (d) was controlled about 150 nm by the milling time. The step angle was adjusted by the incident angle of Ar-ion beam and the rotation angle of the PR mask. After removing the PR mask and Au thin film, the stepped sapphire substrates were annealed in flowing oxygen at 1050 °C for 3 h, in a quartz tube furnace. The substrates were mounted on a heater block using silver paste. CeO₂ buffer layer and *in situ* YBCO thin films were deposited on the stepped sapphire substrates by pulsed laser deposition method. CeO₂ buffer layer was grown typically 15-nm thickness. The YBCO film thickness (t) was varied to obtain the thickness ratio (t/d) of the film to the step height (d) in a range from 0.5 to 1. The YBCO thin film was patterned by Ar ion milling using photolithography, and the Au contact pad was deposited by *rf* sputtering method. Fabricated step edge junction was annealed in flowing oxygen at 500 °C for 1 h. The step edge junction width was obtained by patterning 3, 5, and 10- μ m micro-bridges positioned across the steps. The samples were ultrasonically bonded with aluminum wire onto a sample holder. Superconducting properties of the junctions were measured by using the four-probe method.

III. Results and Discussion

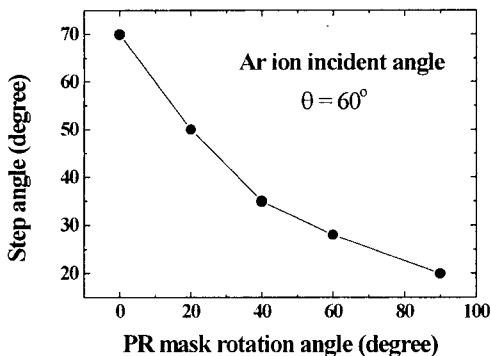


Fig. 1. Control of step angle (α) on sapphire substrate by adjustment of the photoresist mask rotation angle (φ).

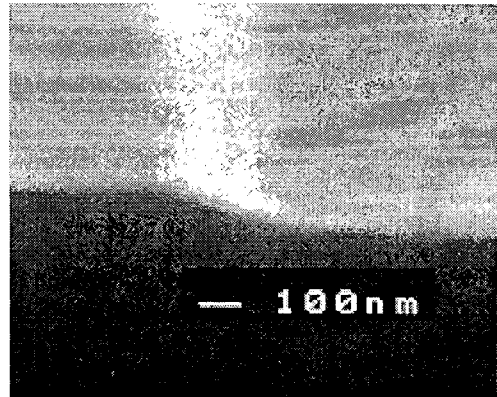


Fig. 2. SEM image of cross section of stepped sapphire substrate after annealing at 1050 °C for 3 h.

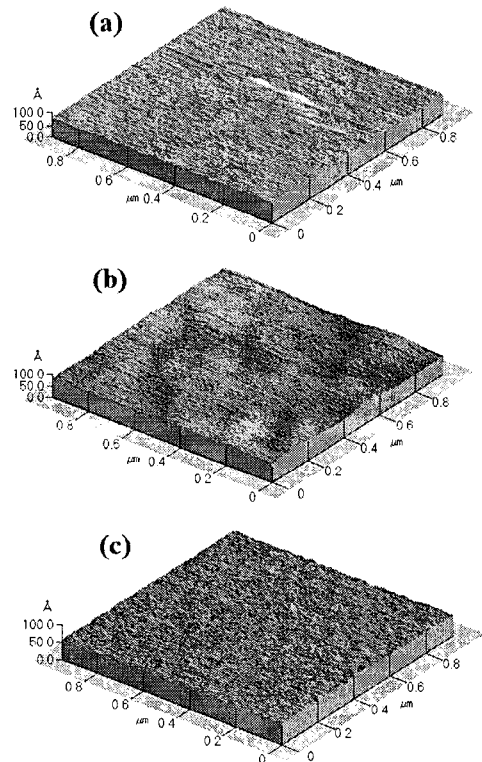


Fig. 3. AFM image of sapphire substrates. (a) commercial substrate, (b) damaged substrate by Ar ion milling process (c) annealed substrate in the flowing oxygen at 1050 °C for 3 h.

High quality YBCO thin films on CeO_2 buffered sapphire substrates were prepared by pulsed laser deposition method with optimized conditions. The patterned YBCO thin films with 10- μm width and 5-mm length exhibit $T_C \geq 89$ K, $\Delta T_C \leq 0.5$ K, and $J_C \geq 3 \times 10^6$ A/cm² [22]. The step angle (α) were controlled adjusting both the incident angle (θ) of Ar ion and the rotation angle (ϕ) of photoresist mask to the incident Ar ion beam. Figure 1 shows the dependence of step angle on PR mask rotation angle with fixed Ar ion incident angle of 60°. The step angle determined from cross sectional SEM images of the step were in the 75°~20° when the rotation angle of PR mark were changed from 0° to 90° with the fixed tilt angle of 60°. The step angle gradually decreased with increasing PR mask angle. Especially, the step angle was controlled from 20° to 35° at the PR mask rotation angle ($\geq 45^\circ$). The SEM image of the cross section of the stepped sapphire substrates after annealing in a flowing oxygen at 1050 °C for 3 h is shown in Figure 2. The stepped sapphire substrate was not reactive of redeposition and backspattering. This leads to the clean and straight step edge fabricated on the sapphire substrates. The roughness of the sapphire surface examined using atomic force microscopy (AFM). Figure 3 shows AFM image of sapphire substrate for the commercial, damaged, and annealed substrates. A commercial

sapphire substrate was examined to have a peak-to-peak roughness of 5~6 Å. The roughness of damaged sapphire substrate by Ar ion milling and annealed sapphire substrates after milling process were measured ~25 Å and ~3 Å, respectively. Therefore, it is regarded that during oxygen annealing process, the damaged substrate surface is recovered successfully.

From now, let us compare the transport properties of step edge junctions for various step edge angles. Step edge junction fabricated in the low step angle ($\leq 40^\circ$) showed a good junction properties with RSJ -like behavior at 77 K. Junction fabricated in high step angles ($\geq 50^\circ$) measured only a normal resistance over 50 Ω . Figure 4 shows a typical I - V curve of YBCO step edge junction of 3- μm -wide, 5- μm -wide and 10- μm -wide junctions fabricated onto the same step line of sapphire substrates with a step angle of 35°. $I_C R_N$ product of the junction is measured about 250 μV . I - V curves show a sharper transition without thermal rounding for the higher step angle than for the lower step angle.

Figure 5 shows the critical current (I_C) and normal resistance (R_N) dependence on the varying thickness ratio (t/d) with step angles of 35°. Normal resistance increases with decreasing the t/d , while the critical current of junction decreases. YBCO micro-bridges formed on lower thickness ratio ($t/d < 0.5$) exhibit no junction behavior, but zero resistance in the I - V measurement at 77 K. The 5- μm width junction

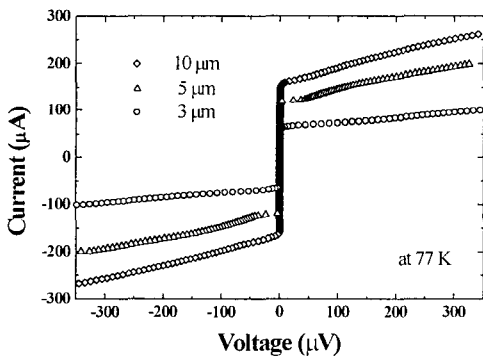


Fig. 4. I - V curves of YBCO step edge junctions of 3, 5, and 10 μm junction width fabricated on same line step measure at 77 K.

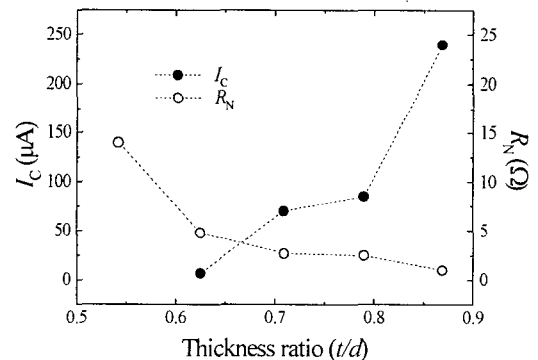


Fig. 5. Critical current and normal resistance dependence on the varying thickness ratio of YBCO thin film with step angle of 35°.

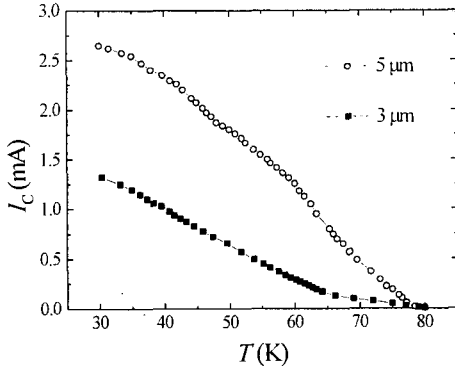


Fig. 6. Temperature dependence of critical current of the YBCO step edge junctions fabricated on junction width of 3 and 5 μm and step angle of 35°. For the junction width of 5 and 3 μm , critical current of junction measured 60 μA and 30 μA at 77 K, normal resistance showed 4.5 Ω and 8 Ω , respectively.

exhibit $I_C R_N$ product of 250 μV for the thickness ratio of 0.8.

Figure 6 shows temperature dependence of critical current in the step edge junctions with junction widths of 3 and 5 μm . Critical current of junction was increased linearly, as temperature is decreased. For the junction width of 5 and 3 μm , critical current measured 60 μA and 30 μA at 77 K, and normal resistance measured 4.5 Ω and 8 Ω , respectively. Normal resistances of junctions were constant 4.5 Ω and 8 Ω over the wide temperature range of 30 K–80 K. Yi et al. [10] reported that the $I_C R_N$ product increased linearly and R_N remained almost constant with to the decreasing temperature for step edge junctions fabricated on LaAlO_3 substrates. YBCO thin film grain boundary junctions and junction with artificial barriers show a scaling $I_C R_N \propto (J_C)^P$, where $P \approx 0.5$ [23]. Figure 7 shows scaling behavior of various step-edge junctions fabricated on sapphire substrates in the wide range of thickness ratio and step angle.

IV. Conclusion

We have fabricated YBCO step-edge junctions on sapphire substrates with CeO_2 buffer layer. The step

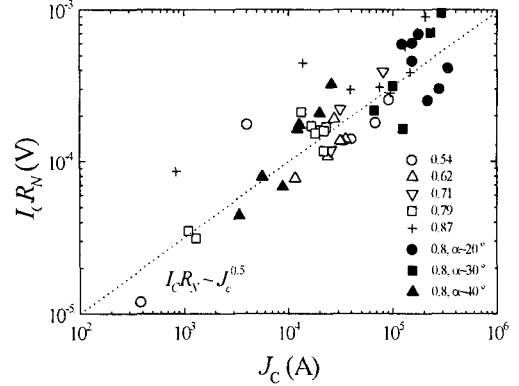


Fig. 7. Scaling behavior of step edge junction fabricated on sapphire substrates: (open) YBCO thickness ratio of 0.54, 0.62, 0.71, 0.79, and 0.89 to the 35° step angle, (solid) step angle of 20°, 30°, and 40°.

angle determined from cross sectional SEM images of the step were in the 75°–20° when the rotation angle of PR mark were changed from 0° to 90° with the fixed tilt angle of 60°. We have compared the transport properties of step edge junctions for various step angle and YBCO thickness ratio. I - V curves of junction fabricated on the thickness ratio of ~ 0.8 and the step angle of 35° were exhibited RSJ -like behavior with $I_C R_N$ product of $\sim 250 \mu\text{V}$ and critical current density of $\sim 2 \times 10^4 \text{ A/cm}^2$ at 77 K. Critical current of step edge junction was increased linearly with decreasing temperature, but the normal resistance was almost constant. Total samples of step edge Josephson junction was satisfied the scaling behavior of the junctions.

References

- [1] G. Friedl, B. Roas, M. Romheld, L. Schultz, and W. Jutz, "Transport properties of epitaxial $\text{YBa}_2\text{Cu}_3\text{O}_x$ films at step edges", *Appl. Phys. Lett.* **59**, 2751-2753 (1991).
- [2] J. A. Edwards, J. S. Satchell, N. G. Chew, N. G. Chew, R. G. Humphreys, M. N. Keene, and O. D. Dosser, "YBa₂Cu₃O₇ thin-film step junction on MgO substrates", *Appl. Phys. Lett.* **60**, 2433-2435 (1992).
- [3] C. W. Yuan, A. B. Berezin, and A. L. de Lozanne,

- “Step edge $\text{YBa}_2\text{Cu}_3\text{O}_7$ dc SQUIDs on sapphire substrates”, *Appl. Phys. Lett.* **60**, 2552-2554 (1992).
- [4] J. Luine, J. Bulman, J. Burch, K. Daly, A. Lee, C. Pettiette-Hall, S. Schwarzbeek, and D. Miller, “Characteristics of high performance $\text{YBa}_2\text{Cu}_3\text{O}_7$ step-edge junctions”, *Appl. Phys. Lett.* **61**, 1128-1130 (1992).
- [5] C. L. Jia, B. Kabius, K. Urban, K. Herrmann, J. Schubert, W. Zander, and A. I. Brabinski, “The microstructure of epitaxial $\text{YBa}_2\text{Cu}_3\text{O}_7$ films on steep steps in LaAlO_3 substrates”, *Physica C* **196**, 211-226 (1992).
- [6] J. Z. Sun, W. J. Gallagher, A. C. Callegari, V. Foglietti, and R. H. Koch, “Improved process for high- T_c superconducting step-edge junctions”, *Appl. Phys. Lett.* **63**, 1561-1563 (1993).
- [7] D. Grudler, R. Eckart, B. David, and O. Dossel, “Origin of 1/f noise in $\text{YBa}_2\text{Cu}_3\text{O}_7$ step-edge dc SQUIDs”, *Appl. Phys. Lett.* **62**, 2134-2136 (1993).
- [8] F. Schmidl, L. Alff, R. Gross, K.-D. Husemann, H. Schneidewind, and P. Seidel, “Superconducting Transports Properties of Step-edge Josephson Junctions”, *IEEE Trans. on Applied Superconductivity* **3**, 2349-2352 (1993).
- [9] A. B. Berezin, C. W. Yuan, and A. L. de Lozanne, “YBCO dc SQUIDs Utilizing Sapphire Step Edge Junctions”, *IEEE Trans. on Applied Superconductivity* **3**, 2457-2460 (1993).
- [10] H. R. Yi, Z. G. Ivanov, D. Winkler, Y. N. Zhang, H. Olin, and P. Larsson, “Improved step edges on LaAlO_3 substrate by using amorphous carbon etch masks”, *Appl. Phys. Lett.* **65**, 1177-1179 (1994).
- [11] J. Ramos, M. Seitz, G. M. Daalmans, D. Uhl, G. Ivanov, and T. Cleason, “Noise properties of single-layer $\text{YBa}_2\text{Cu}_3\text{O}_7$ step-edge DC SQUID’s on MgO substrate”, *Physica C* **220**, 50-54 (1994).
- [12] K. Herrmann, G. Kunkel, M. Siegel, J. Schubert, W. Zander, A. I. Blaginski, C. L. Jia, B. Kabius, and K. Urban, “Correlation of step-edge junction characteristics with microstructure”, *J. Appl. Phys.* **78**, 1131-1139 (1995).
- [13] H. R. Yi, M. Gustafsson, D. Winkler, E. Olsson, and T. Claeson, “Electromagnetic and microstructural characterization of $\text{YBa}_2\text{Cu}_3\text{O}_7$ step edge junction on (001) LaAlO_3 substrates”, *J. Appl. Phys.* **79**, 9213-9220 (1996).
- [14] K. Char, N. Newman, S. M. Garrison, R. W. Barton, R. C. Taber, S. S. Laderman, and R. D. Jacowitz, “Microwave surface resistance of epitaxial $\text{YBa}_2\text{Cu}_3\text{O}_7$ thin films on sapphire”, *Appl. Phys. Lett.* **57**, 409-411 (1990).
- [15] A. B. Berezin, C. W. Yuan, and A. L. de Lozanne, “ $\text{YBa}_2\text{Cu}_3\text{O}_{7-x}$ thin films grown on sapphire with epitaxial MgO buffer layers”, *Appl. Phys. Lett.* **57**, 90-91 (1990).
- [16] B. F. Cole, G.-C. Liang, N. Newman, K. Char, G. Zaharchuk, and J. S. Martens, “Larger-area $\text{YBa}_2\text{Cu}_3\text{O}_{7-\delta}$ thin films on sapphire for microwave applications”, *Appl. Phys. Lett.* **61**, 1727-1729 (1992).
- [17] M. Schieber, M. Schwartz, G. Koren, and E. Aharoni, “Organometallic chemical vapor deposited layers of stabilized zirconia on sapphire as a substrate for laser ablated $\text{YBa}_2\text{Cu}_3\text{O}_{7-x}$ thin films”, *Appl. Phys. Lett.* **58**, 301-303 (1991).
- [18] X. D. Wu, R. E. Muenchausen, N. S. Norgar, A. Pique, R. Edwards, B. Wilkens, T. S. Ravi, D. M. hwang, and C. Y. Chen, “Epitaxial yttria-stabilized zirconia on (1102) sapphire for $\text{YBa}_2\text{Cu}_3\text{O}_{7-\delta}$ thin films”, *Appl. Phys. Lett.* **58**, 304-306 (1991).
- [19] A. Knierim, R. Auer, J. Geenk, G. Linker, O. Meyer, H. Reiner, and R. Schneider, “High critical current densities of $\text{YBa}_2\text{Cu}_3\text{O}_{7-x}$ thin films on buffered technical substrates”, *Appl. Phys. Lett.* **70**, 661-663 (1997).
- [20] X. D. Wu, R. C. Dye, R. E. Muenchausen, S. R. Foltyn, M. Maley, A. D. Rollett, A. R. Garcia, and N. S. Norgar, “Epitaxial CeO_2 films as buffer layers for high-temperature superconducting thin films”, *Appl. Phys. Lett.* **58**, 2165-2167 (1991).
- [21] M. W. Denhoff, and J. P. McCaffrey, “Epitaxial $\text{Y}_1\text{Ba}_2\text{Cu}_3\text{O}_7$ thin films on CeO_2 buffer layers on sapphire substrates”, *J. Appl. Phys.* **70**, 3986-3988 (1991).
- [22] I.-S. Kim, H.-R. Lim, D. H. Kim, and Y. K. Park, “Surface Morphology and Critical current Density of High Quality $\text{YBa}_2\text{Cu}_3\text{O}_7$ Thin Films on Sapphire Substrates”, *IEEE Trans. on Magnetics* **35**, 4073-4075 (1999).
- [23] D. Koelle, R. Kleiner, F. Ludwig, E. Dantsker, and John Clarke, “High-Transition temperature superconducting quantum interference devices”, *Reviews of Modern Physics* **71**, 631-686 (1999)